

Hadronic dissipative effects on elliptic flow in ultrarelativistic heavy-ion collisions

Tetsufumi Hirano,^{1,*} Ulrich Heinz,² Dmitri Kharzeev,³ Roy Lacey,⁴ and Yasushi Nara⁵

¹*Department of Physics, Columbia University, 538 West 120th Street, New York, NY 10027, USA*

²*Department of Physics, Ohio State University, 191 West Woodruff Avenue, Columbus, OH 43210, USA*

³*Nuclear Theory Group, Physics Department, Brookhaven National Laboratory, Upton, NY 11973-5000, USA*

⁴*Department of Chemistry, SUNY Stony Brook, Stony Brook, NY 11794-3400, USA*

⁵*Institut für Theoretische Physik, J. W. Goethe-Universität, Max v. Laue Str. 1, D-60438 Frankfurt, Germany*

(Dated: February 9, 2020)

We study the elliptic flow coefficient $v_2(\eta, b)$ in Au+Au collisions at $\sqrt{s} = 200$ A GeV as a function of pseudorapidity η and impact parameter b . Using a hybrid approach which combines early ideal fluid dynamical evolution with late hadronic rescattering, we demonstrate strong dissipative effects from the hadronic rescattering stage on the elliptic flow. With Glauber model initial conditions, hadronic dissipation is shown to be sufficient to fully explain the differences between measured v_2 values and ideal hydrodynamic predictions. Initial conditions based on the Color Glass Condensate model generate larger elliptic flow and seem to require additional dissipation during the early quark-gluon plasma stage in order to achieve agreement with experiment.

PACS numbers: 25.75.-q, 25.75.Nq, 12.38.Mh, 12.38.Qk

One of the important new discoveries made at the Relativistic Heavy Ion Collider (RHIC) is the large elliptic flow v_2 in non-central Au+Au collisions [1]. At the highest RHIC energy of $\sqrt{s} = 200$ A GeV, the observed v_2 values near midrapidity ($|\eta| \lesssim 1$), for not too large impact parameters ($b \lesssim 7$ fm) and transverse momenta ($p_T \lesssim 1.5$ GeV/c), agree with predictions from ideal fluid dynamics [2], including [3, 4] the predicted dependence of v_2 on the transverse momentum p_T and hadron rest masses [5]. From these observations it has been concluded [6] that in these collisions a quark-gluon plasma (QGP) is created which thermalizes on a very rapid time scale $\tau_{\text{therm}} < 1$ fm/c and subsequently evolves as an almost ideal fluid with exceptionally low viscosity.

On the other hand, the ideal fluid dynamical description gradually breaks down as one studies collisions at larger impact parameters and at lower energies [7] or moves away from midrapidity [8, 9, 10]. This has been attributed alternatively to incomplete thermalization of the QGP during the early stages of the expansion [11] (“early viscosity”) and/or to dissipative effects during the late hadronic expansion stage [12, 13, 14] (“late viscosity”). It has recently been argued [13, 15] that quantum mechanics imposes a lower limit on the shear viscosity *of any medium*, but that the shear viscosity of the QGP can not exceed this lower limit by a large factor [16]. On the other hand, qualitative arguments were presented in Ref. [14] which emphasize the importance of hadronic dissipation and support a picture of a “nearly perfect fluid strongly coupled QGP (sQGP) core and highly dissipative hadronic corona” in ultrarelativistic heavy-ion collisions. In the present paper we explore this issue more quantitatively, by trying to answer the question *how much* of the observed deviation of v_2 from the ideal fluid prediction can be attributed to “late viscosity” in the dissipative hadronic phase, and whether or not significant

additional dissipative effects during the early QGP stage are required for a quantitative understanding of the data.

Our study is based on a comparison of a hybrid model, combining an ideal fluid dynamical QGP stage with a realistic kinetic description of the hadronic stage (hadron cascade), with data on the centrality and rapidity dependence of the p_T -integrated elliptic flow $v_2(\eta, b)$ for charged hadrons [17]. We find that with Glauber model initial conditions [18], suitably generalized to account for the longitudinal structure of the initial fireball [19], hadronic dissipation is sufficient to explain the data. On the other hand, initial conditions based on the Color Glass Condensate (CGC) model [20, 21] lead to larger elliptic flows which overpredict the data unless one additionally assumes that the early QGP stage possesses significant shear viscosity, too. Our analysis points to a need for a better understanding of the initial conditions in heavy-ion collisions if one hopes to use experimental data to constrain the QGP viscosity.

A (1+1)-dimensional hydro+cascade model was first proposed in Ref. [22], putting emphasis on radial flow in heavy-ion collisions. It was later extended to 2+1 dimensions for the study of elliptic flow near midrapidity [12, 23]. By combining a hydrodynamic description of the early expansion stage with a hadron transport model at the end we can implement a realistic treatment of the freeze-out process and of viscous effects during the final hadronic phase. Here we extend the above models to full (3+1)-dimensional hydrodynamics [24], in order to be able to study the rapidity dependence of elliptic flow. Let us briefly summarize our model. For the hydrodynamic stage, we solve the conservation laws $\partial_\mu T^{\mu\nu} = 0$ with the ideal fluid decomposition $T^{\mu\nu} = (e+p)u^\mu u^\nu - pg^{\mu\nu}$ (where e and p are energy density and pressure and u^μ is the fluid 4-velocity) in Bjorken coordinates $(\tau, \mathbf{x}_\perp, \eta_s)$ [9]. We neglect the finite (but at RHIC energy very small) net

baryon density. A massless ideal parton gas equation of state (EOS) is employed in the QGP phase ($T > T_c = 170$ MeV) while a hadronic resonance gas model is used at $T < T_c$. When we use the hydrodynamic code all the way to final decoupling, we take into account [10] chemical freezeout of the hadron abundances at $T_{\text{ch}} = 170$ MeV, separated from thermal freezeout of the momentum spectra at a lower decoupling temperature T_{dec} , as required to reproduce the experimentally measured yields [25].

For the hydro+cascade description, a hadronic transport model JAM [26] is employed for the late stage of the expansion. JAM simulates nuclear collisions by individual hadron-hadron collisions. Soft hadron production in hadron-hadron scattering is modeled by exciting hadronic resonances and color strings. Color strings decay into hadrons after their formation time ($\tau \sim 1$ fm/c) according to the Lund string model PYTHIA [28]. Leading hadrons which contain original constituent quarks can scatter within their formation time with other hadrons assuming additive quark cross sections [29]. In the current study, it is initialized with output from the above (3+1)-dimensional hydrodynamics by using the Cooper-Frye formalism [27] (rejecting backward going particles) [12, 23]. We switch from hydrodynamics to the cascade approach at the switching temperature $T_{\text{sw}} = 169$ MeV, i.e. just below the hadronization phase transition.

We here study two types of initial conditions for the evolution. The first, which we call “modified BGK initial condition” [19, 34], assumes an initial entropy distribution of massless partons according to

$$\begin{aligned} \frac{dS}{d\eta_s d^2x_\perp} &= \frac{C}{1+\alpha} \theta(Y_b - |\eta_s|) f^{pp}(\eta_s) \\ &\times \left[\alpha \left(\frac{Y_b - \eta_s}{Y_b} \frac{dN_{\text{part}}^A}{d^2x_\perp} + \frac{Y_b + \eta_s}{Y_b} \frac{dN_{\text{part}}^B}{d^2x_\perp} \right) \right. \\ &\left. + (1-\alpha) \frac{dN_{\text{coll}}}{d^2x_\perp} \right], \end{aligned} \quad (1)$$

where $\eta_s = \frac{1}{2} \ln[(t+z)/(t-z)]$ is the space-time rapidity, $\mathbf{x}_\perp = (x, y)$ is the position transverse to the beam axis, $C = 24.0$ is chosen to reproduce the measured charged hadron multiplicity in central collisions at midrapidity [30], Y_b is the beam rapidity, and f^{pp} is a suitable parametrization of the shape of rapidity distribution in pp collisions,

$$f^{pp}(\eta_s) = \exp \left[-\theta(|\eta_s| - \Delta\eta) \frac{(|\eta_s| - \Delta\eta)^2}{\sigma_\eta^2} \right], \quad (2)$$

with $\Delta\eta = 1.3$ and $\sigma_\eta = 2.1$, which are so chosen as to reproduce the measured pseudorapidity distributions for charged hadrons [31]. $N_{\text{part}}^{A,B}$ and N_{coll} are the number of wounded nucleons in the two nuclei and the number of binary nucleon-nucleon collisions, respectively, as calculated from the Glauber model nuclear thickness function

$T_{A,B}(\mathbf{x}_\perp)$ [18],

$$\frac{dN_{\text{part}}^A}{d^2x_\perp} = T_A(r_+) \left[1 - \left(1 - \frac{\sigma_{NN}^{\text{in}} T_B(r_-)}{B} \right)^B \right], \quad (3)$$

$$\frac{dN_{\text{part}}^B}{d^2x_\perp} = T_B(r_-) \left[1 - \left(1 - \frac{\sigma_{NN}^{\text{in}} T_A(r_+)}{A} \right)^A \right], \quad (4)$$

$$\frac{dN_{\text{coll}}}{d^2x_\perp} = \sigma_{NN}^{\text{in}} T_A(r_+) T_B(r_-), \quad (5)$$

with the inelastic nucleon-nucleon cross section $\sigma_{NN}^{\text{in}} = 42$ mb and $r_\pm = [(x \pm \frac{1}{2}b)^2 + y^2]^{1/2}$ (where b is the impact parameter). The soft/hard fraction $\alpha = 0.85$ was adjusted to reproduce the measured centrality dependence [30] of the charged hadron multiplicity at midrapidity. At $\eta_s = 0$, Eq. (1) reduces to $dS/(d\eta_s d^2x_\perp) \propto [\alpha(N_{\text{part}}^A + N_{\text{part}}^B) + (1-\alpha)N_{\text{coll}}]/(1+\alpha)$ [35]; this parameterization is equivalent to the one used in Ref. [20], $\sim \frac{1-x}{2}(N_{\text{part}}^A + N_{\text{part}}^B) + xN_{\text{coll}}$, with $x = \frac{1-\alpha}{1+\alpha}$. From Eq. (1), we can compute the entropy density at the initial time $\tau_0 = 0.6$ fm/c [2] of the hydrodynamic evolution, $s(\tau_0, \mathbf{x}_\perp, \eta_s) = dS/(\tau_0 d\eta_s d^2x_\perp)$, which provides the initial energy density and pressure distributions through the tabulated EOS described above.

The second type of initial conditions is based on the CGC model [32]. Specifically, we use the Kharzeev-Levin-Nardi (KLN) approach [20] in the version previously employed in [21]. In this approach, the energy distribution of produced gluons with rapidity y is given by the k_T -factorization formula [33]

$$\begin{aligned} \frac{dE_T}{d^2x_\perp dy} &= \frac{4\pi^2 N_c}{N_c^2 - 1} \int \frac{d^2p_T}{p_T} \int^{p_T} d^2k_T \alpha_s(Q^2) \\ &\times \phi_A(x_1, k_T^2; \mathbf{x}_\perp) \phi_B(x_2, (p_T - k_T)^2; \mathbf{x}_\perp), \end{aligned} \quad (6)$$

where $x_{1,2} = p_T \exp(\pm y)/\sqrt{s}$ and p_T is the transverse momentum of the produced gluons. For the unintegrated gluon distribution function we use

$$\phi_A(x, k_T^2; \mathbf{x}_\perp) = \begin{cases} \frac{\kappa C_F}{2\pi^3 \alpha_s(Q_s^2)} \frac{Q_s^2}{Q_s^2 + \Lambda^2}, & k_T \leq Q_s, \\ \frac{\kappa C_F}{2\pi^3 \alpha_s(Q_s^2)} \frac{Q_s^2}{k_T^2 + \Lambda^2}, & k_T > Q_s, \end{cases} \quad (7)$$

where $C_F = \frac{N_c^2 - 1}{2N_c}$ and Q_s denotes the saturation momentum. We introduce a small regulator $\Lambda = 0.2$ GeV/c in order to have a smooth distribution in the forward rapidity region $|y| > 4.5$ at RHIC (other regions are not affected by introducing this small regulator). The overall normalization κ is determined by fitting the multiplicity of charged hadron at midrapidity at $\sqrt{s_{NN}} = 200$ GeV for the most central collisions. The saturation momentum Q_s of nucleus A in $A+B$ collisions, needed in the function ϕ_A , is obtained by solving the following implicit equation at fixed x and \mathbf{x}_\perp :

$$Q_s^2(x, \mathbf{x}_\perp) = \frac{2\pi^2}{C_F} \alpha_s(Q_s^2) x G(x, Q_s^2) \frac{dN_{\text{part}}^A}{d^2x_\perp}. \quad (8)$$

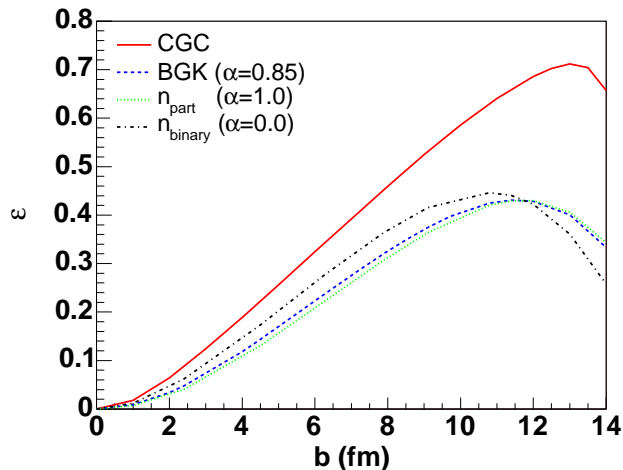


FIG. 1: (Color online) Initial spatial eccentricity $\varepsilon = \frac{\langle y^2 - x^2 \rangle}{\langle y^2 + x^2 \rangle}$ at midrapidity as a function of impact parameter b , for 200 A GeV Au+Au collisions with CGC (solid red) and BGK (dashed blue) initial conditions. For comparison we also show initial conditions where the initial parton density at midrapidity scales with the transverse density of wounded nucleons (dotted green) and of binary collisions (dash-dotted black) [18].

An analogous equation holds for the saturation momentum of nucleus B in ϕ_B . For the gluon distribution function G inside a nucleon we take the simple ansatz [20]

$$xG(x, Q^2) = K \ln \left(\frac{Q_s^2 + \Lambda^2}{\Lambda_{\text{QCD}}^2} \right) x^{-\lambda} (1-x)^4 \quad (9)$$

with $\Lambda = \Lambda_{\text{QCD}} = 0.2 \text{ GeV}$. We choose $K = 0.7$ and $\lambda = 0.2$ so that the average saturation momentum in the transverse plane yields $\langle Q_s^2(x=0.01) \rangle \sim 2.0 \text{ GeV}^2/c^2$ in central 200 A GeV Au+Au collisions at RHIC. For the running coupling constant α_s in Eq. (8) we use the standard perturbative one-loop formula, but introducing a cut-off in the infra-red region of small Q_s (i.e. near the surface of the nuclear overlap region where the produced gluon density is low) by limiting the coupling constant to $\alpha_s \leq 0.5$. We can obtain the energy density distribution at time τ_0 from Eq. (6), $e(\tau_0, \mathbf{x}_\perp, \eta_s) = dE_T / (\tau_0 d\eta_s d^2x_\perp)$, where y is identified with η_s , and use this as the initial distribution for the hydrodynamic evolution.

In Fig. 1 we show the initial eccentricity $\varepsilon = \frac{\langle y^2 - x^2 \rangle}{\langle y^2 + x^2 \rangle}$ of the source at midrapidity ($\eta_s = 0$) for our two models for the initial conditions. Here $\langle \dots \rangle$ represents the average taken with respect to the initial energy density distribution $e(\tau_0, \mathbf{x}_\perp, \eta_s = 0)$. While the BGK model interpolates between the binary collision and wounded nucleon scaling curves (being closer to the latter), CGC initial conditions are seen to give much larger eccentricities. This can be traced back to a steeper drop of the energy density profile

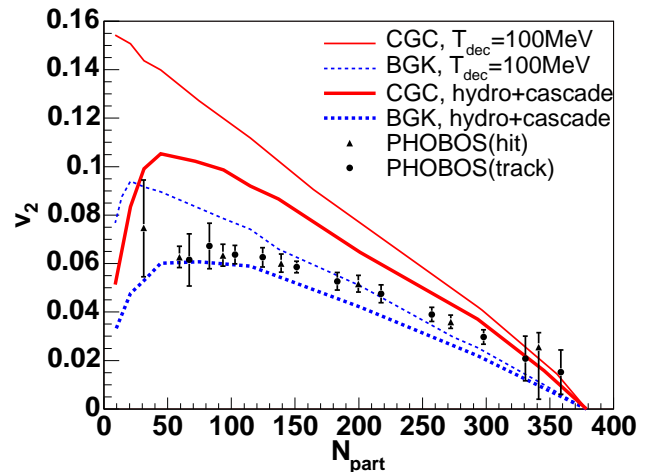


FIG. 2: (Color online) p_T -integrated elliptic flow for charged hadrons at midrapidity ($|\eta| < 1$) from 200 A GeV Au+Au collisions, as a function of the number N_{part} of participating nucleons. The thin lines show the prediction from ideal fluid dynamics with a freeze-out temperature $T_{\text{dec}} = 100 \text{ MeV}$, for CGC (solid red) and BGK (dashed blue) initial conditions. The thick lines (solid red for CGC and dashed blue for BGK initial conditions) show the corresponding results from the hydro+cascade hybrid model. The data are from the PHOBOS Collaboration [17].

near the edge in the CGC model. In ideal fluid dynamics, the larger eccentricities ε result in larger elliptic flow coefficients v_2 .

This is shown by the thin lines in Fig. 2 which compare ideal fluid dynamical calculations with RHIC data from the PHOBOS collaboration [17]. Note that the hydrodynamic calculations shown here use an EOS in which the hadron abundances are held fixed below T_c at their chemical freeze-out values established during the hadronization process [10]. As explained in [14], this results in smaller v_2 values than for a hadronic EOS which assumes hadronic chemical equilibrium all the way down to kinetic freeze-out at T_{dec} . Correspondingly, our curve for BGK initial conditions lies below the one shown in Fig. 2 of [17] which uses the latter EOS. It is noteworthy that for central and semicentral collisions the data seem to lie consistently somewhat above the hydrodynamic predictions with BGK initial conditions. While at first sight this seems to argue against the validity of the BGK model, it must be noted that event-by-event fluctuations in the geometry of the nuclear overlap region, which are not taken into account in our dynamical simulations, tend to significantly increase v_2 in collisions with small impact parameters (large N_{part} values) [36].

The difference between the eccentricities given by the BGK and CGC initial conditions may seem surprising in view of the fact that the centrality dependence of hadron multiplicities in both approaches can be made numeri-

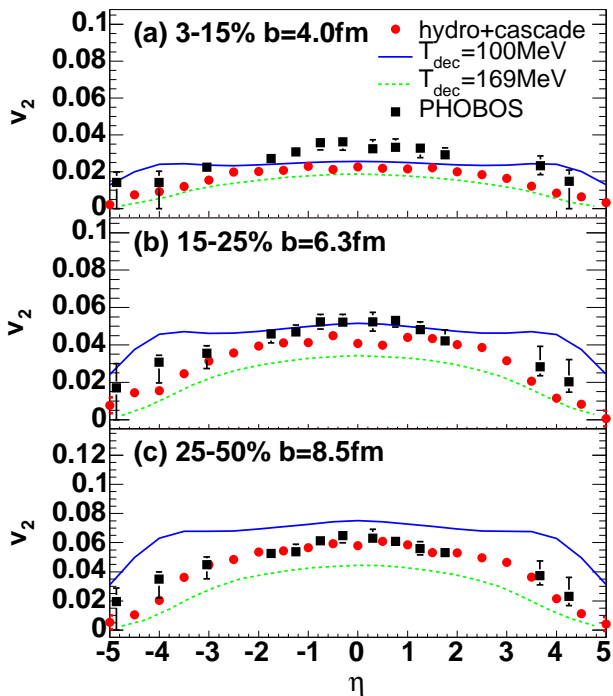


FIG. 3: (Color online) The pseudorapidity dependence of v_2 for charged hadrons in (a) central (3-15%), (b) semicentral (15-25%), and (c) peripheral (25-50%) Au+Au collisions at $\sqrt{s} = 200 A$ GeV. The corresponding impact parameters are, respectively, $b = 4.0, 6.3,$ and 8.5 fm. The hydrodynamic evolution is initialized with modified BGK initial conditions. The lines show the predictions from ideal fluid dynamics with $T_{\text{dec}} = 100$ MeV (solid blue) and $T_{\text{dec}} = 169$ MeV (dashed green). The red circles show the corresponding results from the hydro+cascade hybrid model. The black squares are measurements by the PHOBOS Collaboration [17].

cally very similar by a proper choice of parameter α in Eq. (1) [20]. When parameterized in terms of Eq. (1), the main prediction of the CGC approach is the near independence of α on the collision energy, which is confirmed by the data. The reason for the big difference in the eccentricities stems from the different entropy profiles predicted by the two approaches, especially in the regions where the density of produced particles is relatively small. While these differences contribute little to the total observed multiplicity, they appear quite important for the evaluation of eccentricity. The application of the CGC approach in the region of small parton density is of course questionable, and a better theoretical understanding of the transition from high to low density regimes is clearly needed.

The thick lines show the centrality dependence of v_2 from the hydro+cascade hybrid model. Whereas with BGK initial conditions the dissipative effects of the

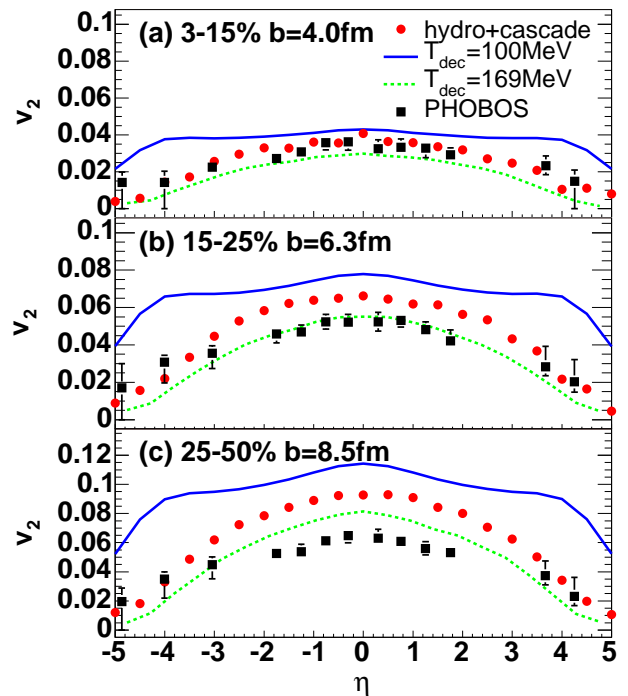


FIG. 4: (Color online) The same as Fig. 3 except for the initial condition taken from the CGC model instead of the BGK model.

hadronic phase in the cascade model reduce the purely hydrodynamic v_2 sufficiently to bring the theory in agreement with the data even for peripheral collisions, CGC initial conditions, with their larger eccentricities, cause so much elliptic flow that even the hybrid model overpredicts the data significantly. With such initial conditions even the QGP phase must exhibit significant dissipative effects if one wants to reproduce the RHIC data.

In Figs. 3 and 4 we show the measured [17] rapidity dependence of v_2 for three centrality classes, together with calculations at three representative impact parameters $b = 4, 6.3$ and 8.5 fm corresponding to these centrality selections (i.e. adjusted to give the correct average number of participants N_{part} in each case as quoted in Ref. [17]). Results from BGK initial conditions are shown in Fig. 3. The lines show ideal fluid dynamical calculations with kinetic decoupling assumed at $T_{\text{dec}} = 100$ MeV (solid blue) and $T_{\text{dec}} = T_{\text{sw}} = 169$ MeV (dashed green). The dashed lines underpredict the data at all impact parameters and all but the most forward rapidities, indicating the need for generating additional elliptic flow during the hadronic stage below T_c . The solid lines, on the other hand, strongly overpredict the forward rapidity data in semiperipheral and peripheral collisions, showing that ideal hydrodynamics generates too much additional elliptic flow

during the hadronic stage. The hydro+cascade hybrid model (red circles) gives a good description of the data over the entire rapidity range for all three centralities, with the exception of the midrapidity region in the most central collision sample as already discussed above. The hadronic cascade model provides just the right amount of dissipation to bring the ideal fluid prediction down to the measured values, especially in very peripheral collisions and away from midrapidity.

The situation is different for the more eccentric CGC initial conditions, as shown in Fig. 4. Now v_2 is over-predicted at all centralities and rapidities if the hadronic phase is described by ideal fluid dynamics, and the dissipative effects of the hadronic cascade are no longer sufficient to reduce v_2 for the more peripheral bins enough to obtain agreement with the data. In the peripheral sample (25-50%) the excess elliptic flow persists at almost all rapidities and exists even if the fireball freezes out directly at hadronization (no hadronic evolution at all). Significant dissipation in the early QGP phase is needed in this case to bring the theoretical prediction in line with experiment.

We conclude that the answer to the question, whether all of the observed discrepancies between elliptic flow data and ideal fluid dynamical simulations can be blamed on “late hadronic viscosity” and fully eliminated by employing a hydro+cascade hybrid model such as the one studied here, depends on presently unknown details of the initial state of the matter formed in the heavy-ion collision. With BGK initial conditions hadronic dissipation seems to be able to reduce the elliptic flow enough to bring the theoretical predictions in line with the data, leaving little room for additional dissipative effects in the early QGP stage. CGC initial conditions yield significantly more eccentric sources and produce larger than observed elliptic flow even if dissipative effects in the late hadronic stage are taken into account. In this case, the early QGP phase must exhibit a significant amount of viscosity, too. With CGC initial conditions, the excess over the v_2 data from Au+Au collisions at RHIC persists even at midrapidity in all but the most central collisions; with such initial conditions, the standard claim [2] that at RHIC energies the measured elliptic flow at midrapidity exhausts the theoretical upper limit predicted by ideal fluid dynamics must be qualified.

We see that a data-based attempt to establish limits on the viscosity of the quark-gluon plasma requires a better understanding of the initial conditions of the fireball created in RHIC collisions. Unfortunately, very few direct probes of the initial conditions are available. In Ref. [19, 37] 3-dimensional jet tomography was proposed to test the longitudinal structure of BGK and CGC initial conditions in noncentral collisions. A specific feature of CGC initial conditions is a predicted sign flip of the first Fourier moment v_1 of nuclear modification factor $R_{AA}(p_T, y, \phi)$ at high p_T as one moves away from midra-

pidity [37]. Alternatively, one can try to exploit the fact that the large (even if not perfect) degree of thermalization observed in heavy-ion collisions at RHIC limits the amount of entropy produced during the expansion. When taking into account that final state rescatterings in the medium produce only very small effects on the shape of the rapidity distribution, the finally observed charged hadron rapidity distributions therefore severely constrain the initial entropy and energy density profiles [20]. A better theoretical understanding of the initial conditions, especially of the transition from the high density to small density regimes, is needed to extract the viscosity of quark-gluon plasma at the early stages. A systematic study of the charged hadron rapidity distributions for a variety of collision centralities, center of mass energies and system sizes is needed to assess which description of the initial state yields a more consistent and efficient overall description of all available data.

This work was supported by the U.S. DOE under contracts DE-FG02-93ER40764 (T.H.), DE-FG02-01ER41190 (U.H.), DE-AC02-98CH10886 (D.K.) and DE-FG02-87ER40331.A008 (R.L.). Discussions with A. Adil, M. Gyulassy, and A.J. Kuhlman are gratefully acknowledged.

* Correspond to hirano@phys.columbia.edu

- [1] The experimental situation is summarized in B.B. Back *et al.* [PHOBOS Collaboration], Nucl. Phys. **A 757**, 28 (2005); J. Adams *et al.* [STAR Collaboration], Nucl. Phys. **A 757**, 102 (2005); K. Adcox *et al.* [PHENIX Collaboration], Nucl. Phys. **A 757**, 184 (2005).
- [2] For a theoretical review see P.F. Kolb and U. Heinz, in *Quark-Gluon Plasma 3*, edited by R.C. Hwa and X.-N. Wang (World Scientific, Singapore, 2004), p. 634 [nucl-th/0305084].
- [3] C. Adler *et al.* [STAR Collaboration], Phys. Rev. Lett. **87**, 182301 (2001); J. Adams *et al.* [STAR Collaboration], Phys. Rev. Lett. **92**, 052302 (2001).
- [4] K. Adcox *et al.* [PHENIX Collaboration], Phys. Rev. Lett. **89**, 212301 (2002); S.S. Adler *et al.* [PHENIX Collaboration] Phys. Rev. Lett. **91**, 182301 (2003).
- [5] P. Huovinen, P.F. Kolb, U. Heinz, P.V. Ruuskanen, and S.A. Voloshin, Phys. Lett. B **503**, 58 (2001).
- [6] U. Heinz and P.F. Kolb, Nucl. Phys. **A 702**, 269c (2002); M. Gyulassy and L.D. McLerran, Nucl. Phys. **A 750**, 30 (2005); E.V. Shuryak, Nucl. Phys. **A 750**, 64 (2005).
- [7] C. Adler *et al.* [STAR Collaboration], Phys. Rev. C **66** 034904 (2002); C. Alt *et al.* [NA49 Collaboration], Phys. Rev. C **68**, 034903 (2003).
- [8] B.B. Back *et al.* [PHOBOS Collaboration], Phys. Rev. Lett. **89**, 222301 (2002)
- [9] T. Hirano, Phys. Rev. C **65**, 011901 (2002).
- [10] T. Hirano and K. Tsuda, Phys. Rev. C **66**, 054905 (2002).
- [11] U. Heinz and P.F. Kolb, J. Phys. G **30**, S1229 (2004).
- [12] D. Teaney, J. Lauret, and E.V. Shuryak, nucl-th/0110037.
- [13] M. Gyulassy, nucl-th/0403032.

- [14] T. Hirano and M. Gyulassy, nucl-th/0506049.
- [15] P. Kovtun, D.T. Son and A.O. Starinets, Phys. Rev. Lett. **94**, 111601 (2005); G. Policastro, D.T. Son and A.O. Starinets, Phys. Rev. Lett. **87**, 081601 (2001).
- [16] D. Teaney, Phys. Rev. C **68**, 034913 (2003).
- [17] B.B. Back *et al.* [PHOBOS Collaboration], nucl-ex/0407012
- [18] P.F. Kolb, U. Heinz, P. Huovinen, K.J. Eskola and K. Tuominen, Nucl. Phys. A **696**, 197 (2001).
- [19] A. Adil and M. Gyulassy, Phys. Rev. C **72**, 034907 (2005).
- [20] D. Kharzeev and M. Nardi, Phys. Lett. B **507**, 121 (2001); D. Kharzeev and E. Levin, *ibid.* B **523**, 79 (2001); D. Kharzeev, E. Levin and M. Nardi, Phys. Rev. C **71**, 054903 (2005); D. Kharzeev, E. Levin and M. Nardi, Nucl. Phys. A **730**, 448 (2004).
- [21] T. Hirano and Y. Nara, Nucl. Phys. A **743**, 305 (2004).
- [22] A. Dumitru, S.A. Bass, M. Bleicher, H. Stoecker and W. Greiner, Phys. Lett. B **460**, 411 (1999); S.A. Bass, A. Dumitru, M. Bleicher, L. Bravina, E. Zabrodin, H. Stoecker and W. Greiner, Phys. Rev. C **60**, 021902 (1999); S.A. Bass and A. Dumitru, Phys. Rev. C **61**, 064909 (2000).
- [23] D. Teaney, J. Lauret and E.V. Shuryak, Phys. Rev. Lett. **86**, 4783 (2001).
- [24] C. Nonaka and S.A. Bass, nucl-th/0510038. [This paper employs different hydrodynamic and hadronic cascade codes from the present paper.]
- [25] P. Braun-Munzinger, D. Magestro, K. Redlich and J. Stachel, Phys. Lett. B **518**, 41 (2001).
- [26] Y. Nara, N. Otuka, A. Ohnishi, K. Niita and S. Chiba, Phys. Rev. C **61**, 024901 (2000).
- [27] F. Cooper and G. Frye, Phys. Rev. D **10**, 186 (1974).
- [28] T. Sjöstrand *et al.*, Comp. Phys. Comm. **135**, 238 (2001).
- [29] H. Sorge, Phys. Rev. C **52**, 3291 (1995); S.A. Bass *et al.*, Prog. Part. Nucl. Phys. **41**, 255 (1998).
- [30] B.B. Back *et al.* [PHOBOS Collaboration], Phys. Rev. C **65**, 061901 (2002).
- [31] B. B. Back *et al.*, Phys. Rev. Lett. **91**, 052303 (2003).
- [32] L.D. McLerran and R. Venugopalan, Phys. Rev. D **49**, 2233 (1994); **49**, 3352 (1994); **50**, 2225 (1994).
- [33] L.V. Gribov, E.M. Levin, and M.G. Ryskin, Phys. Rept. **100**, 1 (1983); E. Laenen and E. Levin, Ann. Rev. Nucl. Part. Sci. **44**, 199 (1994).
- [34] S.J. Brodsky, J.F. Gunion and J.H. Kuhn, Phys. Rev. Lett. **39**, 1120 (1977).
- [35] A.J. Kuhlman and U. Heinz, Phys. Rev. C **72**, 037901 (2005). [This paper uses a slightly smaller soft fraction $\alpha = 0.75$.]
- [36] M. Miller and R. Snellings, nucl-ex/0312008.
- [37] A. Adil, M. Gyulassy and T. Hirano, nucl-th/0509064.